Random Dopant Fluctuation Modelling with the Impedance Field Method

Andreas Wettstein*, Oleg Penzin†, Eugeny Lyumkis† and Wolfgang Fichtner‡
*ISE Integrated Systems Engineering AG, Balgriststrasse 102, CH-8008 Zürich, Switzerland,
E-mail: wettstein@ise.ch
†ISE Integrated Systems Engineering, Inc., 111 N. Market St., San Jose, CA 95113, USA
‡Institut für Integrierte Systeme, ETH Zürich, CH-8092 Zürich, Switzerland

***Abstract*— We discuss an approach for the modelling of random dopant fluctuations based on the impedance field method that has been recently integrated into DESSIS [1]. The method is easy to use and orders of magnitudes more efficient than the statistical method.**

I. Introduction

As devices become smaller, self-averaging of device properties for individual devices becomes less effective. Therefore, for small devices, the statistical variations of device properties are important. This paper is concerned with one important source of variations: random dopant fluctuations (RDFs).

The conventional numerical approach to RDFs is to run a large number of simulations on devices that differ microscopically (this is called the 'statistical method'). Often, device samples result from a Monte Carlo process simulation in which each dopant atom is treated individually [2]–[4]. As the doping comes from a process simulator, the statistical properties of the dopant distribution are accounted for automatically. A severe shortcoming of this method is the huge numerical expense, caused by the necessity to run many 3D simulations. Treating individual dopants as point charges causes singularities in the potential. Different remedies to this problem have been suggested (for example, splitting the potential in a short-range and long-range term [2], or modifying the mobility [3]), but the size of the error introduced by these workarounds is unclear.

II. Theory

In this paper, we discuss an alternative to model RDFs. The method (in a slightly different formulation) was proposed first in Ref. [5]. For each point in the device, we describe the RDFs by the second-order statistical moments of the dopant distribution function, and model these moments by an analytical function. Assuming that the local fluctuations are small, we can compute the fluctuations of the terminal characteristics using the impedance field method, which is familiar from noise modelling [6]. We now outline the method. To make the connection to noise more obvious, we include a frequency dependence in the analysis. As the random dopant fluctuations are static, for the purpose of this paper, $\omega = 0$ is sufficient.

A. Impedance field method

The device equations read:

$$\begin{aligned}
&\nabla\epsilon(\vec{r})\cdot\nabla\phi(\vec{r}) = e\left[n(\vec{r}) - N(\vec{r})\right] \quad \text{for } \vec{r}\in\Omega\\
&\nabla\cdot\vec{j}_n(\vec{r}) = eR\left[n(\vec{r})\right] + i\omega n(\vec{r}) \quad \text{for } \vec{r}\in\Omega\\
&\vec{j}_n(\vec{r}) = \mu_n\left[k_{\mathrm{B}}T\nabla n(\vec{r}) - en(\vec{r})\nabla\phi(\vec{r})\right]\\
&\hat{n}(\vec{r})\cdot\nabla\phi(\vec{r}) = 0 \quad \text{for } \vec{r}\in\partial\Omega\setminus\cup_k C^k\\
&\hat{n}(\vec{r})\cdot\vec{j}_n(\vec{r}) = 0 \quad \text{for } \vec{r}\in\partial\Omega\setminus\cup_k C^k\\
&\int_{C^k}\mathrm{d}^2\hat{n}\cdot\vec{j}_n(\vec{r}) = I_k\\
&\phi(\vec{r}) = V_k + \phi_{\mathrm{bi}}(\vec{r}) \quad \text{for } \vec{r}\in C^k\subset\partial\Omega\\
&n(\vec{r}) = n_0(\vec{r}) \quad \text{for } \vec{r}\in C^k\subset\partial\Omega
\end{aligned} \tag{1}$$

n, $\vec{j}_n$, ϕ, T, and N denote the electron density, electron current density, electrostatic potential, temperature, and doping concentration, respectively. $\vec{r} = (x, y, z)$ is the position coordinate, $\hat{n}$ is the unit vector normal to the boundary, Ω is the computational domain, and C^k is the k-th contact. The quantities ϕ_{bi} and n_0 are given. Only half of the values for the contact voltages V_k and contact currents I_k can be prescribed, the others come out as results. For brevity, we omit the equations for holes. Including them is straightforward, as is adding equations for temperatures or quantum corrections, imposing more complicated boundary conditions, or using more sophisticated models for the dielectric constant ϵ, the recombination rate R, or the electron mobility μ_n.

We add a small perturbation δN to the doping concentration N. Denoting the response of the density and potential as δn and $\delta\phi$, we linearise (1):

$$\begin{aligned}
&\nabla\epsilon(\vec{r})\cdot\nabla\delta\phi(\vec{r}) = e\left[\delta n(\vec{r}) - \delta N(\vec{r},\omega)\right] \quad \text{for } \vec{r}\in\Omega\\
&\nabla\cdot\delta\vec{j}_n = e\frac{\partial R\left[n(\vec{r})\right]}{\partial n(\vec{r})}\delta n(\vec{r}) + i\omega\delta n(\vec{r}) \quad \text{for } \vec{r}\in\Omega\\
&\delta\vec{j}_n(\vec{r}) = \mu_n\left[k_{\mathrm{B}}T\nabla\delta n - e\delta n\nabla\phi - en\nabla\delta\phi\right]\\
&\hat{n}(\vec{r})\cdot\nabla\delta\phi(\vec{r}) = 0 \quad \text{for } \vec{r}\in\partial\Omega\setminus\cup_k C^k\\
&\hat{n}(\vec{r})\cdot\delta\vec{j}_n(\vec{r}) = 0 \quad \text{for } \vec{r}\in\partial\Omega\setminus\cup_k C^k\\
&\int_{C^k}\mathrm{d}^2\hat{n}\cdot\delta\vec{j}_n(\vec{r}) = \delta I_k\\
&\delta\phi(\vec{r}) = \delta V_k \quad \text{for } \vec{r}\in C^k\subset\partial\Omega\\
&\delta n(\vec{r}) = 0 \quad \text{for } \vec{r}\in C^k\subset\partial\Omega
\end{aligned} \tag{2}$$

 0-7803-7826-1/03/$17.00 © 2003 IEEE

Again, in order to obtain a unique solution, we can prescribe only as many values for δV_k and δI_k as there are contacts; the others come out as results.

Here, we demand $\delta I_k = 0$ and compute δV_k. As (2) is linear in the perturbations, δV_k is a linear function of δN:

$$\delta V_k(\omega) = \int_\Omega \mathrm{d}^3 r G_k(\vec{r},\omega)\,\delta N(\vec{r},\omega)$$

A discretised version of the Green function G can be easily obtained from the complex Jacobian of the discretised equation system. We have to solve a matrix similar to this Jacobian for a single right-hand side. Therefore, computing G takes no more time than a few Newton steps.

For RDF analysis, δN is the deviation of the doping in a particular device from the average doping N. Therefore, the statistical average of δN vanishes, $\langle \delta N \rangle = 0$. Then, in our linear approximation $\langle \delta V_k \rangle = 0$ also, and new information is only obtained from higher order statistical moments,

$$S_V^{ij} = \int_\Omega \mathrm{d}^3\vec{r}_i \mathrm{d}^3\vec{r}_j G_i(\vec{r}_i,\omega)\,K(\vec{r}_i,\vec{r}_j,\omega)\,G_j^*(\vec{r}_j,\omega) \ , \quad (3)$$

where the noise voltage spectrum S_V^{ij} is a second-order moment defined as $S_V^{ij}(\omega) = \left\langle \delta V_i \delta V_j^* \right\rangle(\omega)$.

B. Noise source: model for dopant fluctuation correlations

For the noise source K, we need a physical model. As the doping is static, K vanishes for $\omega \neq 0$. Furthermore, we assume that individual dopants are placed randomly and independently (according to a Poisson distribution) with a probability given by their average local concentration. Therefore, the second-order moment of the doping distribution is

$$K(\vec{r}_i,\vec{r}_j,\omega) = N_{\mathrm{tot}}(\vec{r}_i)\,\delta(\vec{r}_i - \vec{r}_j)\,2\pi\delta(\omega) \ , \quad (4)$$

where N_{tot} is the average total doping concentration. (Note that the moments of acceptors and donors add, rather than compensate.) Assuming that the dopants are spatially uncorrelated simplifies (3) significantly, as one of the integrations drops out due to the δ-function.

C. Quasi-2D problems

In practice, we often consider devices that are wide and nearly homogeneous in one spatial direction z. We can simulate them in 2D and take their z-extension into account only by scaling the results with their width L_z. We now show that this remains possible for RDF analysis, even when δN is highly inhomogeneous in z.

For a device homogeneous in z, we can write $\Omega = \Omega_2 \times [0, L_z]$, where Ω_2 is the projection of the domain in the xy-plane. Similarly, $C^k = C_2^k \times [0, L_z]$. Furthermore, homogeneity in z means that neither n_0 nor ϕ_{bi} in (1) depends explicitly on z. As a result, the solution (n, ϕ) is independent of z as well. For the linearised equation system (2), the only z-dependence is in the perturbations δn, $\delta\vec{j}$, $\delta\phi$, and δN.

When we average (2) over z, we obtain equations of the same form. The perturbations are replaced by their z-averages, and ∇ by the 2D derivative $(\partial/\partial x, \partial/\partial y)$ (the z-component drops out due to the Neumann boundary conditions at $z = 0$ and $z = L_z$). The averaged equations completely determine δV_k in terms of the 2D function $\overline{\delta N}$, the z-average of δN,

$$\delta V_k = \int_{\Omega_2} \mathrm{d}x\mathrm{d}y G_k^{\mathrm{2D}}(x,y,\omega)\,\overline{\delta N}(x,y,\omega) \ , \quad (5)$$

where G_k^{2D} is the Green function obtained from solving the z-averaged system. From (4) and (5), we obtain

$$S_V^{ij} = \int_\Omega \mathrm{d}^3\vec{r} \frac{G_i^{\mathrm{2D}}(x,y,\omega)}{L_z} N_{\mathrm{tot}}(x,y)\,2\pi\delta(\omega)\,\frac{G_j^{\mathrm{2D}^*}(x,y,\omega)}{L_z}.$$

As the z-integration only contributes a factor L_z, we immediately see that $S_V^{ij} \propto L_z^{-1}$. Furthermore, comparison to (3) shows that $G_i(\vec{r},\omega) = G_i^{\mathrm{2D}}(x,y,\omega)/L_z$. RDFs for a 3D problem homogeneous in z therefore can be fully analysed in 2D, without additional approximations.

III. Discussion

Dopants interact during the diffusion steps of device processing. Hence, the assumption that the dopants are uncorrelated is questionable. In principle, the impedance field method is able to handle spatial correlations. However, the additional integral needed to evaluate (3) has a high numerical cost unless the correlation length is small compared to the device size. Due to the lack of appropriate models, we do not consider spatial correlations here. Our model in (4) has the plausible property that the absolute value of fluctuation increases with doping density, but the relative value decreases. We assume that this is already sufficient to obtain reasonable results.

The most important assumption in our method is that the fluctuations are small, which allows to linearise the problem. The actual problem here is the smallness of the solution variable response $(\delta n, \delta\phi)$, as the perturbation of the doping δN indeed does enter the Poisson equation linearly. In parts of the device where the free carrier concentration is low, we expect the variation in the free carrier densities to matter only slightly, and the assumption of linearity to hold. On the other hand, in regions with many free carriers, the dopants are well screened, and the doping fluctuations effectively look small.

As distant points in devices are uncorrelated, we can imagine that a very wide device is made up of a large number $Z \propto L_z$ of independent, narrower devices connected in parallel. The statistical law of large numbers requires that $S_V^{ij} \propto Z^{-1}$. Hence, for large L_z, any physically reasonable model must yield $S_V^{ij} \propto L_z^{-1}$. As shown in Section II-C, our approach preserves this fundamental statistical feature, which further increases our confidence in its ability to provide meaningful results.

IV. Results

To demonstrate the application of the impedance field method to RDFs, we investigate the drain current I_{D} and its standard deviation $\sigma_{I_{\mathrm{D}}}$ for a simple MOSFET as a function of gate voltage V_{G}. To this end, we convert the noise voltage

 0-7803-7826-1/03/$17.00 © 2003 IEEE

spectrum to a noise current spectrum using the admittance matrix Y and then transform it back to the time domain:

$$\sigma_I^2(t) = \int \frac{d\omega}{2\pi} \exp(-i\omega t)\, Y(\omega)\, S_V(\omega)\, Y^H(\omega)$$

In this case, we consider the drain to be the only port and, therefore, the matrices in the equation above are plain numbers. As $S_V \propto \delta(\omega)$, the t-dependence disappears.

The simulation was performed in 2D and the width L_z of the device was accounted for by proper scaling. Fig. 1 shows relative standard deviation $\sigma_{I_\mathrm{D}}/I_\mathrm{D}$. As $S_V \propto L_z^{-1}$, $I_\mathrm{D} \propto L_z$, and $Y \propto L_z$, we scaled the curve with $\sqrt{L_z}$ to make it independent of L_z.

For comparison, we performed naive 2D statistical simulations for different L_z. In this approach, for each dopant species and for each vertex i in the 2D mesh, we determine the average number $\langle M_i \rangle = \langle N_i \rangle A_i L_z$ of dopants in the 3D volume associated with the vertex, based on the area A_i of 2D box i and the average dopant concentration $\langle N_i \rangle$ in the box. $\langle M_i \rangle$ parameterises the Poisson distribution function P used to randomly pick the actual number of dopants M_i (and the dopant concentration $N_i = M_i/A_i L_z$) in the box:

$$P(M_i) = \frac{\exp(-\langle M_i \rangle)}{M_i!} \langle M_i \rangle^{M_i}$$

The variance of the Poisson distribution function is $\sigma_{M_i}^2 = \langle M_i \rangle \propto L_z$. Therefore, if the equation system (1) was linear, we would obtain $\sigma_{I_\mathrm{D}} \propto \sqrt{L_z}$; as it is not linear, deviations are possible. (The law of large numbers does not apply, as in our statistical approach the fluctuations are artificially correlated in z-direction.) While our statistical approach is unphysical, it allows us to investigate the nonlinearity, using the same 2D mesh for all simulations, therefore avoiding the problem of eliminating meshing-related effects from our results.

Fig. 1 shows the results obtained from 50 runs for each device width. For the devices with $L_z = 10\,\mu\mathrm{m}$ and $L_z = 1\,\mu\mathrm{m}$, the agreement to the impedance field method is excellent. For $L_z = 0.1\,\mu\mathrm{m}$, small deviations occur. However, the shape of the curve remains the same.

To use RDF analysis to predict the fraction of devices that deviate from the average too much to be usable, we must predict how big the tails of the distribution functions are. It is not immediately obvious that the variances provide enough infomation about these tails. In Fig. 2, we show the fraction $h(I_\mathrm{D})$ of runs of our statistical simulations that yielded a drain current of at most I_D. For easier comparison, we plot h as a function of the normalised quantity $(I_\mathrm{D} - \langle I_\mathrm{D} \rangle)/\sigma_{I_\mathrm{D}}$ rather than as a function of I_D. If the current fluctuations were Gaussian and for an infinite number of samples, we would observe

$$h(I_\mathrm{D}) = \frac{1}{\sigma_{I_\mathrm{D}}\sqrt{2\pi}} \int_{-\infty}^{I_\mathrm{D}} \mathrm{d}I \exp\left[-\frac{1}{2}\left(\frac{I - \langle I_\mathrm{D} \rangle}{\sigma_{I_\mathrm{D}}}\right)\right] .$$

Fig. 2 shows that for all values of L_z, our statistical samples are well approximated by a Gaussian. As the Gauss distribution function is fully determined by $\langle I_\mathrm{D} \rangle$ and σ_{I_D}, the second-order moment is sufficient to describe the entire distribution function, including the tails. (In principle, the impedance field method is capable to compute higher order statistical moments also. For local correlations, the numerical cost remains small.)

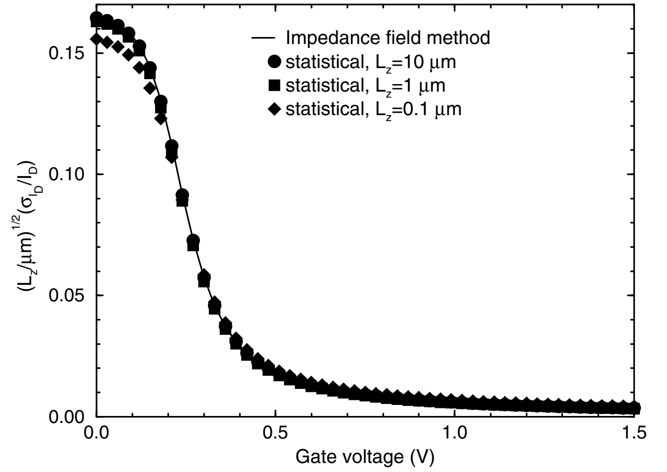

Fig. 1. Device width–scaled relative standard deviation of drain current I_D versus gate voltage, obtained from the 2D impedance field method and 2D statistical simulations with various scaling factors L_z. The channel length of the device was $100\,\mathrm{nm}$, the oxide thickness was $3\,\mathrm{nm}$, the channel doping concentration was $5 \cdot 10^{17}\,\mathrm{cm}^{-3}$, and the drain voltage $V_\mathrm{D} = 50\,\mathrm{mV}$. To simplify comparison, all simulations used a doping-independent mobility.

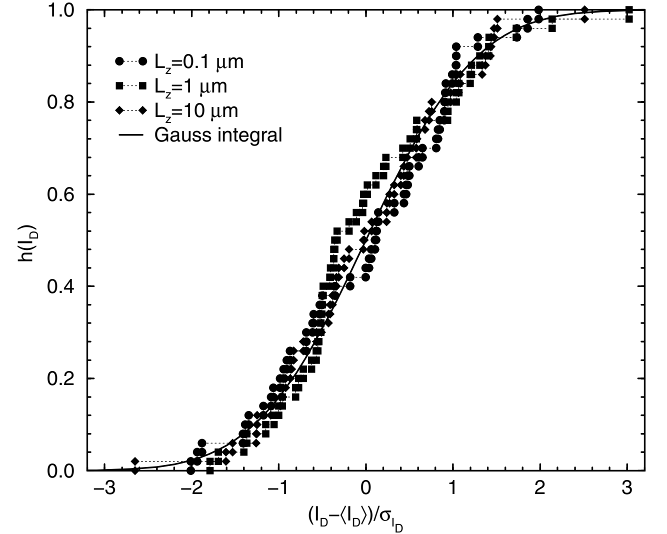

Fig. 2. Fraction $h(I_\mathrm{D})$ of runs of our statistical simulations that yielded currents of at most I_D. The device and biases were identical to those for Fig. 1, and $V_\mathrm{G} = 0.3\,\mathrm{V}$.

Both analytical models and numerical experiments using the statistical method show that the standard deviation of the threshold voltage scales with the channel length L_G as $1/\sqrt{L_\mathrm{G}}$ [4]. (This is another manifestation of the statistical law of large numbers, as discussed in Section III for the L_z-scaling.) To demonstrate this behaviour with our model, we computed the standard deviation of the gate voltage σ_{V_G} as a function of the gate voltage V_G. We assumed that drain voltage V_D and drain current I_D are fixed and, therefore, the entire effect of

0-7803-7826-1/03/$17.00 © 2003 IEEE

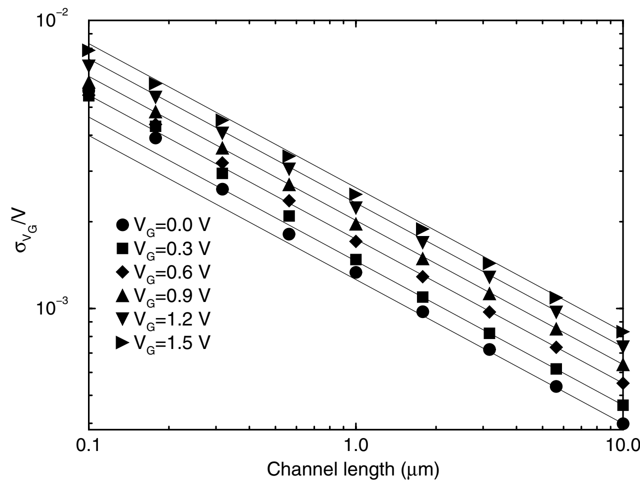

Fig. 3. Gate voltage fluctuation as a function of $L_{\rm G}$. All devices were $1\,\mu$m wide, and had an oxide thickness of $3\,$nm, a channel doping of $5{\cdot}10^{17}\,{\rm cm}^{-3}$, and source/drain doping of $10^{20}\,{\rm cm}^{-3}$. $V_{\rm D}$ and $I_{\rm D}$ were fixed with respect to RDFs; the average $V_{\rm D} = 50\,$mV. The lines are $1/\sqrt{L_{\rm G}}$ extrapolations from the $10\,\mu$m data points.

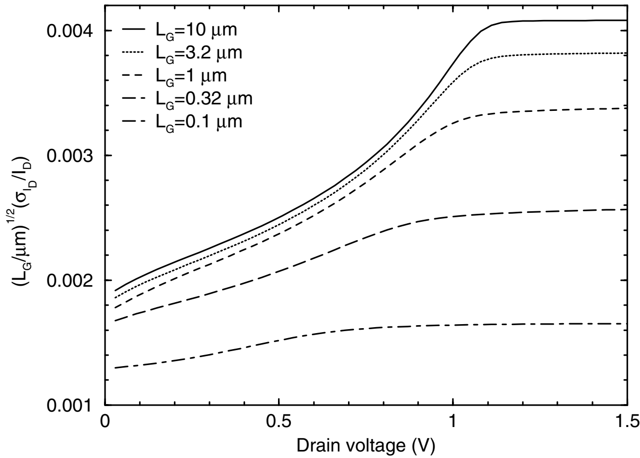

Fig. 4. Channel length–scaled relative fluctuation of the drain current as a function of drain voltage for the devices from Fig. 3 for $V_{\rm G} = 1.5\,$V.

the RDFs was transferred to the gate. The results are shown in Fig. 3. For long channel devices, the $1/\sqrt{L_{\rm G}}$ behaviour holds for the entire range of gate voltages (and, therefore, also for the threshold voltage). For short channels, the gate voltage fluctuation does not follow the $1/\sqrt{L_{\rm G}}$ law. This is to be expected, as the relative contributions of the channel become smaller for smaller devices. The fluctuations are in the same order of magnitude as obtained from the statistical method [4].

Fig. 4 shows the $\sqrt{L_{\rm G}}$-scaled relative standard deviation of the drain current, $\sigma_{I_{\rm D}}\sqrt{L_{\rm G}}/I_{\rm D}$, as a function of drain voltage $V_{\rm D}$ for large gate voltage $V_{\rm G} = 1.5\,$V. For small $V_{\rm D}$, the relative fluctuations increase with $V_{\rm D}$ and then saturate. The $1/\sqrt{L_{\rm G}}$ law holds only for very large $L_{\rm G}$. Fig. 5 shows the local noise voltage spectral density (LNVSD) for the drain voltage fluctuations $\sigma_{V_{\rm D}}$ for the $L_{\rm G} = 1\,\mu$m device (the

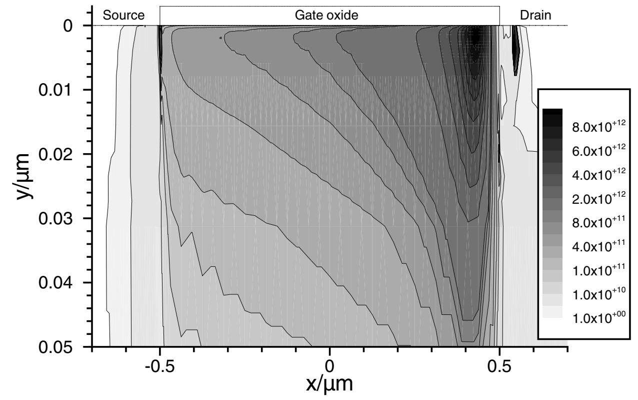

Fig. 5. Drain LNVSD for the $L_{\rm G} = 1\,\mu$m device from Fig. 3 for $V_{\rm D} = V_{\rm G} = 1.5\,$V. The contour lines are labelled in units of ${\rm V}^2{\rm s}/{\rm cm}^3$.

integral of this quantity over device is $\sigma^2_{V_{\rm D}}$). Clearly, for this channel length, the non-uniformity along the channel is still so dominant that the $1/\sqrt{L_{\rm G}}$-scaling cannot hold.

V. Conclusion

We discussed RDF analysis based on the impedance field method. While the linearisation inherent to the method is not justified from a theoretical point of view, our numerical experiments do not indicate any severe problems. The linearisation circumvents the problems that arise in statistical simulations from the highly localised donor charges.

We demonstated that the statistical fluctuations of the terminal currents are Gaussian and, therefore, well characterised by the second-order moments. The method is, therefore, suitable for yield analysis, where the interest is with devices that deviate greatly from the average.

The impedance field method is much faster than statistical methods and can be easily embedded into existing DESSIS simulation projects, using the same physical parameters and the same meshes as for the simulation of other properties. Those properties make the method suitable for routine simulations in an industrial environment.

References

[1] *DESSIS Technical Manual*, Release 9.0, ISE Integrated Systems Engineering AG, Balgriststrasse 102, CH-8008 Zürich, 2003.

[2] T. Ezaki, T. Ikezawa, A. Notsu, K. Tanaka, and M. Hane, “3D MOSFET simulation considering long-range Coulomb potential effects for analyzing statistical dopant-induced fluctuations associated with atomistic process simulator,” in *SISPAD 2002 Proceedings*. Kobe: Business Center for Academic Societies, Japan, Sept. 2002, pp. 91–94.

[3] A. Asenov, M. Jaraiz, S. Roy, G. Roy, F. Adamu-Lema, A. R. Brown, V. Moroz, and R. Gafiteanu, “Integrated atomistic process and device simulation of decananometre MOSFETs,” in *SISPAD 2002 Proceedings*. Kobe: Business Center for Academic Societies, Japan, Sept. 2002, pp. 87–90.

[4] Y. Oda, Y. Ohkura, K. Suzuki, S. Ito, H. Amakawa, and K. Nishi, “Statistical fluctuation analysis by Monte Carlo ion implantation method,” in *SISPAD 2002 Proceedings*. Kobe: Business Center for Academic Societies, Japan, Sept. 2002, pp. 199–202.

[5] I. D. Mayergoyz and P. Andrei, “Statistical analysis of semiconductor devices,” *J. Appl. Phys.*, vol. 90, no. 6, pp. 3019–3029, Sept. 2001.

[6] F. Bonani, G. Ghione, M. R. Pinto, and R. K. Smith, “An efficient approach to noise analysis through multidimensional physics-based models,” *IEEE Trans. Electron Devices*, vol. 45, no. 1, pp. 261–269, Jan. 1998.

 0-7803-7826-1/03/$17.00 © 2003 IEEE